Soils and Foundations 2015;55(6):1441–1453

HOSTED BY

ELSEVIER

CrossMark

The Japanese Geotechnical Society

Soils and Foundations

www.sciencedirect.com
journal homepage: www.elsevier.com/locate/sandf

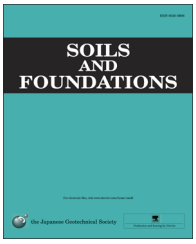

Aging effects on the mechanical property of waste mixture in coastal landfill sites

Lan Chau Nguyen[a,*], Toru Inui[b,1], Kazuki Ikeda[c,2], Takeshi Katsumi[b,3]

[a]Civil Engineering Department, University of Transport and Communications, LangThuong, DongDa, Hanoi, Vietnam
[b]Graduate School of Global Environmental Studies, Kyoto University, Yoshida-Honmachi, Sakyo-ku, Kyoto 606-8501 Japan
[c]Formerly Department of Urban Management, Graduate School of Engineering, Kyoto University, Japan

Received 4 July 2014; received in revised form 4 July 2015; accepted 29 August 2015
Available online 2 December 2015

Abstract

Coastal landfill sites not only offer an option for disposal but also create a new land space after the completion of landfilling. To perform proper design on settlement, stability, and/or bearing capacity at landfill sites, the geotechnical properties of the waste layer such as deformation and shear strength should be investigated. This research is focused on the mechanical properties of waste mixture sampled at a coastal landfill site including municipal solid waste incinerator ash, slag, soil and others, to provide useful information on geotechnical properties in utilizing coastal landfill sites after their closure. A series of triaxial consolidated undrained compression tests (CU) and hydraulic conductivity tests were carried out on the reconstituted waste samples before and after being cured in simulated leachate water in coastal landfill sites for different periods, to understand the aging effects on mechanical properties of waste mixture. It was shown that while curing results in an increase in the peak strength and deformation modulus, the residual strength was not affected by the curing periods. Scanning electron microscope observations and X-ray diffraction analysis on the waste samples after curing confirmed that the formation of ettringite and hydration products had a densification effect on the microstructure. The higher peak shear strength and lower hydraulic conductivity of the waste samples were attributed to this effect.

Keywords: Waste layer; Curing time; Coastal landfill; Triaxial test; Mechanical property; Ettringite

1. Introduction

Coastal landfilling is an important method for disposal of municipal solid waste incinerator ash (MSWIA), slag, soil, and others in Japan. According to the Ministry of the Environment, Japan, approximately 20% MSW was disposed of in coastal landfill sites, and the weight ratio of MSWIA in landfilled wastes reached almost 78% in 2003 (Shimaoka et al. 2007). In general, coastal landfill sites are located at strategic points in the port areas of Tokyo, Nagoya and Osaka with relatively easy access from the metropolitan areas. Coastal landfill reclamation is a key option considering the limited land available in Japan. For this reason, it is important to investigate the strength, bearing capacity, and deformation properties of the waste mixture layers deposited in the coastal landfill. However, limited research regarding the geotechnical properties of the waste mixture layers in coastal landfill sites has been carried out, and the engineering properties of waste mixtures, which include incinerator ash, slag, and surplus soil, remain largely unknown. However, studies have been carried out in

*Corresponding author. Tel.: +84 912 533 480; fax: +81 75 753 5116.
E-mail addresses: nguyenchaulan@utc.edu.vn (L.C. Nguyen), inui.toru.3v@kyoto-u.ac.jp (T. Inui), kazukichi800@gmail.com (K. Ikeda), katsumi.takeshi.6v@kyoto-u.ac.jp (T. Katsumi).
[1]Tel.: +81 75 753 5752; fax: +81 75 753 5116.
[2]Tel.: +81 75 753 5114; fax: +81 75 753 5116.
[3]Tel.: +81 75 753 9205; fax: +81 75 753 5116.
Peer review under responsibility of the Japanese Geotechnical Society.

http://dx.doi.org/10.1016/j.sandf.2015.10.009

the framework of the Osaka Bay Phoenix Project, which is an extensive coastal landfill project that started in 1990 and has 45 million m3 of total capacity, geotechnical investigations were carried out for the MSW landfill zone at Amagasaki offshore disposal site to determine its physical and dynamic properties (Aburatani et al. 1996). This research concluded that the wet unit weight of the waste layer varied between 15 and 18 kN/m3, depending on the depth of waste layer, the internal friction angle ranged from 24.5° to 35°, and mechanical properties of the MSW-reclaimed layers were equivalent to those of loose alluvial sandy soil with an average SPT-N value of 4.5.

Another important but poorly studied aspect is the time dependency on the waste mixture properties, particularly the changes in geotechnical properties of the waste mixture with time in coastal landfill sites. Sato et al. (2001) conducted consolidated drained triaxial tests on MSW incinerator ash specimens, which were cured under three different conditions including dry, wet and submerged conditions. The results showed an increase in the strength of the MSW incinerator ash samples with the longer curing periods due to the hydration and pozzolanic reactions. An increase in the shear strength in the incinerator ash samples that were submerged in water was also reported by Itoh et al. (2005) and Towhata et al. (2010). These previous works indicated that reduction in the pore space and decrease in the hydraulic conductivity occurred by the curing effects. A study carried out on the MSWIA cured in a fully-sealed condition by Doi et al. (2000) showed that the unconfined compression strength increased with time, while hydraulic conductivity decreased by two orders of magnitude together with a reduction in the compressibility of MSWIA. The authors pointed out that ettringite generation and cementation with time influenced these mechanical properties.

Considering that MSWIA is a major landfilled waste in Japan, these previous studies suggest the importance of considering the aging effects on the geotechnical properties of waste mixtures submerged in landfill leachate or seawater. However, there have been few works that evaluate the shear strength and deformation properties of the waste mixture when it interacts with actual or simulated coastal landfill leachate for a long time. In this study, waste mixture immediately before being disposed of in a coastal landfill site was collected, and reconstituted specimens were cured in simulated leachate for different time periods to simulate the interactions with the leachate in a coastal landfill site. A series of triaxial consolidated undrained (CU) compression tests and hydraulic conductivity tests were carried out on the specimens before and after being cured. Scanning electron microscope (SEM) and X-ray diffraction (XRD) analyzes were also conducted to further understand of the changes in the microstructures of waste mixture. Based on these experimental results and observations, the aging effects on the mechanical properties and microstructures of the waste mixture reclaimed in coastal landfills were discussed.

2. Materials and methods

2.1. Material

The waste mixture used in this study was collected at a coastal landfill site in Osaka Bay area, Japan, immediately before reclamation. The composition of the waste mixture collected was approximately 50% of MSWIA, 30% of gravel materials like slags, and 20% surplus soil, based on the waste acceptance record. Approximately 200 kg of the wet waste mixture was collected and then air-dried in a laboratory at a constant temperature of 20 °C. After that, large pieces of debris such as glass and rocks were removed and the mixture was sieved with a 9.5 mm opening sieve. The sample after sieving was considered the mixture of MSWIA and soil containing small slags and gravels (Table 1).

Fig. 1 shows the particle size distribution of the waste mixture sample after sieving, determined according to JIS A 1204 (2009). The grain size distribution indicates this waste mixture is composed of 85.9 % sand fraction (> 0.075 mm), 8.1% silt fraction (0.005–0.075 mm) and 6.0% clay fraction (< 0.005 mm). The uniformity and curvature coefficients were 127.8 and 2.63, respectively. The material was well graded with a particle size distribution corresponding to SG-F (gravely sand with fine fraction), according to the JGS 0051 (2009). The specific gravity of the waste mixture sample was 2.67. The chemical composition of the waste sample determined by the X-ray florescence spectroscopy (XRF) is shown in Table 2. The XRF shows that calcium oxide is the main component (51.6% in CaO), which indicates a certain hydration ability of the sample. Fig. 2 shows the compaction curve of the waste mixture, according to the A–c method of Standard Proctor Compaction Test, JIS A 1210 (2009).

Table 1
Chemical composition of the waste mixtures sample.

Chemicals	CaO	Fe_2O_3	SiO_2	Al_2O_3	TiO_2	SO_3	K_2O	ZnO	Others
Content (%)	51.6	20.4	9.1	4.3	3.3	2.8	1.7	1.9	4.9

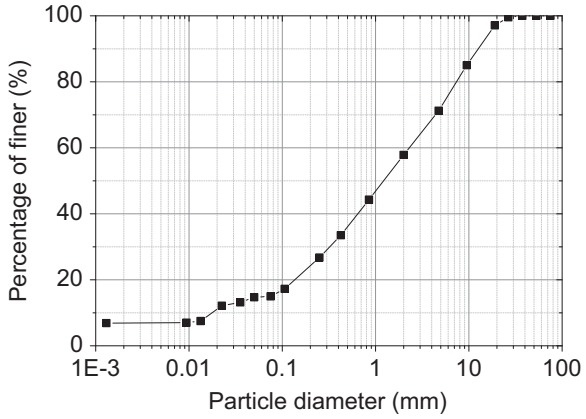

Fig. 1. Particle size distribution of the waste mixture sample after sieving.

Table 2
Conditions and results of CU triaxial compression tests

Sample ID	Curing period (day)	Confining pressure σ_c (kPa)	Dry density before curing (g/cm^3)	Dry density after curing (g/cm^3)	B-value (–)	Peak deviator stress, q_p (kPa)	Axial strain at q_p (%)	Specific gravity before curing	Specific gravity after curing
A1		50	1.02		0.95	242.6	15.0	2.67	
A2	0	100	1.02		0.95	276.8	14.9	2.67	
A3		150	1.02		0.95	320.3	14.9	2.67	
B1		50	1.02	–	–	360.2	8.0	–	–
B2	7	100	1.02	–	0.95	388.9	5.6	–	–
B3		150	1.02	–	0.96	411.1	8.0	–	–
B4		50	1.02	1.02	0.95	329.5	10.1	2.67	2.66
B5	14	100	1.03	1.03	0.95	393.9	15.0	2.66	2.66
B6		150	1.02	–	0.94	429.2	8.3	–	–
B7		50	1.02	–	0.98	373.4	12.0	–	–
B8	28	100	1.03	–	0.96	427.9	10.1	–	–
B9		150	1.02	–	0.95	438.6	13.7	–	–
B10		50	1.02	1.03	0.95	357.8	14.8	2.66	2.67
B11	60	100	1.02	1.04	0.95	416.5	8.0	2.66	2.68
B12		150	1.02	–	0.97	444.3	9.6	–	–
B13		50	1.02	1.09	0.95	401.6	15.0	2.67	2.70
B14	90	100	1.02	1.03	0.95	448.8	15.0	2.67	2.69
B15		150	1.02	1.09	0.95	485.5	15.0	2.67	2.67
B16		50	1.02	1.02	0.97	355.5	15.0	2.67	2.71
B17	120	100	1.03	1.03	0.98	458.0	7.2	2.67	2.68
B18		150	1.02	1.03	0.95	486.0	7.2	2.67	2.7
B19		50	1.02	1.04	0.96	410.5	8.1	2.67	2.71
B20	150	100	1.02	1.06	0.95	500.3	14.4	2.67	2.71
B21		150	1.02	1.17	0.97	630.6	10.2	2.67	2.69
B22		50	1.02	1.26	0.95	493.9	10.7	2.67	2.72
B23	180	100	1.02	1.05	0.95	546.3	11.6	2.67	2.70
B24		150	1.02	1.10	0.95	612.5	5.3	2.67	2.69

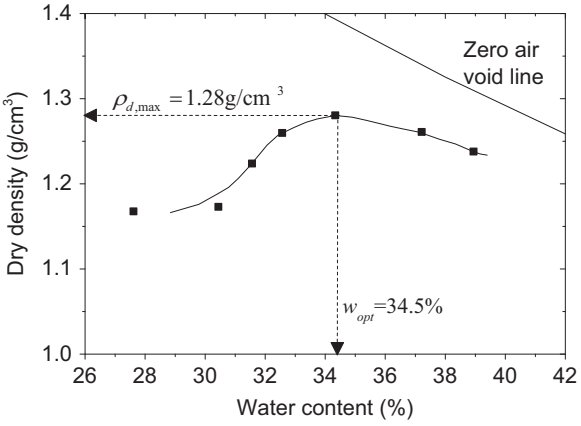

Fig. 2. Proctor compaction curve for the waste mixture sample.

To prepare a simulated leachate with a chemical composition equivalent to that of the leachate in a coastal landfill site which could be used for the submerged curing of the specimens, 30 L of seawater was collected in Osaka Bay, and then mixed with the waste mixture sample in a tank, with the weight ratio of the waste mixture to seawater of 0.1. The mixture was stirred daily for 7 days and then was filtered through a sieve of 75 μm opening. After that, the calcium concentration and the pH of the simulated leachate were measured, at 1,850 mg/L and 7.95, respectively. To simulate the aging effects in a coastal landfill site, the specimens were cured in the simulated leachate for up to 180 days.

2.2. Methods

2.2.1. Preparation of waste mixture specimens

Araike et al. (2010) reported that in situ saturated density of waste mixture reclaimed in the coastal landfill site of Osaka Bay is approximately 1.6 Mg/m^3. The waste mixture was prepared with its optimum water content and degree of compaction of 80%, which is equivalent to the saturated density of 1.6 Mg/m^3. In this study, 27 specimens were prepared and tested in total. All the specimens were prepared by compacting in 5 layers into a split cylindrical mold (50 mm in diameter and 100 mm in height) with its degree of compaction of 80% (ρ_d = 1.02 Mg/m^3) and optimum water content of 34.5%.

CU tests were conducted for two series of specimens: series A (A1–A3) for samples without curing and series B (B4–B24) for samples that were cured in seawater for certain periods. For series A, CU and hydraulic conductivity tests were conducted immediately after preparing specimens. For series B, samples were prepared as follows:

1) Samples were compacted in a split steel mold in the manner explained above.
2) Each specimen was transferred from the mold into a split acrylic mold (50 mm diameter and 100 mm in height).
3) Filter papers and porous disks were fixed on the top and bottom surfaces of the specimen in an acrylic mold to allow water intake and drainage during curing, but not to allow volume expansion.
4) Specimens were submerged in the simulated leachate, which was de-aired for 24 h in a vacuum desiccator to facilitate saturation.
5) Saturated specimens were cured in the simulated leachate under an average room temperature of 20 ± 2 °C for 7, 14, 28, 60, 90, 120, 150, or 180 days.

2.2.2. CU tests and hydraulic conductivity tests

Consolidated-undrained triaxial tests with pore water pressure measurements were carried out on waste mixture specimens by following JGS 0523 (2009). The specimens were prepared following JGS 0520 (2009), and saturated by applying a vacuum procedure under a constant effective confining pressure of 20 kPa (Rad and Clough 1984). After reaching the final step (-70 kPa for cell pressure and -90 kPa for back pressure), de-aired water was circulated into the specimen for 3 h and then back pressure and cell pressure were reduced to –20 kPa and 0 kPa, respectively. Back pressure and cell pressure were increased step by step until they reached 220 kPa and 240 kPa, respectively. After that, whether the specimen had a pore pressure coefficient (B-value) higher than 0.95 was checked to ensure that specimen were fully saturated.

According to the Ministry of the Environment, Japan, approximately 90% of coastal landfills in Japan have reclamation depths of less than 15 m. Considering that the wet unit weight of waste layer was about 17 kN/m^3 above water table and 16 kN/m^3 below water table, which lies in 2 m below the ground level at the coastal landfill site of Osaka Bay (Araike et al. 2010), the effective overburden pressure at 5 m, 10 m and 15 m depth were approximately 53 kPa, 84 kPa and 115 kPa. With the assumption that the lateral effective pressure was equal to the vertical effective pressure, the confining pressures, σ_c, of 50, 100, and 150 kPa were employed in the triaxial tests. After each specimen was consolidated with a designated effective confining pressure, it was compressed at a constant axial strain rate of 0.5%/min until the cumulative axial strain reached 15%. The axial strain was measured by a DDP-50A displacement transducer (Tokyo Sokki Kenkyujo Co., Ltd.) with a capacity of 50 mm, and was automatically recorded by a data logger. Test conditions and physical properties of the specimens for the CU tests are summarized in Table 2.

Hydraulic conductivity tests were conducted on the waste mixture specimens set up in a triaxial compression cell with a falling headwater-constant tailwater system (see in Fig. 3). First, the specimen with 100 mm height and 50 mm diameter was saturated by using a double negative pressure method which was employed in CU tests. Second, the constant cell pressure of 30 kPa was kept without applying any back pressure to conduct the hydraulic conductivity test under the effective confining pressure of 30 kPa. Water head loss across the test specimen and effluent volume during permeation was periodically measured and recorded to calculate the hydraulic conductivity. The test was terminated when the changes in hydraulic conductivity values with time were negligible.

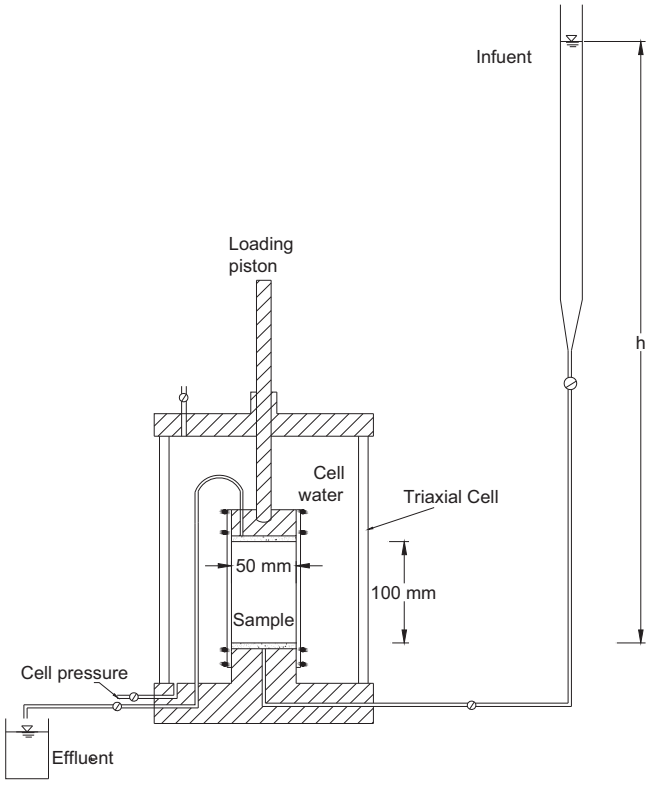

Fig. 3. Schematic setup of hydraulic conductivity tests by using the triaxial testing apparatus.

2.2.3. XRD and SEM analyzes

The mineralogical structure of the waste mixture specimens after curing were analyzed by a X-ray diffractometer (RAD-2B, Rigaku Corporation, using a Cu target with a Ni filter and input energy of 40 kV and 20 mA). After running the CU triaxial test, the specimens were stored at a constant temperature of 30 ± 3 °C in an oven for 24 h for air-drying. Then, a piece of each specimen around the core was taken and grounded to powder with a maximum particle size smaller than 75 μm. The powder-state sample was analyzed by XRD with the diffraction angle (2 theta) ranging from 3° to 40°.

Fragments of 5 mm^3 from the specimens subjected to the triaxial test were air-dried at 30 ± 0.1 °C in an oven for 24 h. Then the SEM device (JSM-5510 LV, JEOL) was used to observe the microstructure of the specimens. SEM images were taken at magnifications of 100–5000 to identify crystallization and other chemical reactions due to curing through visual observations.

3. Results and discussions

3.1. CU tests

3.1.1. Relationship between stress–strain and pore water pressure

The peak deviator stress, q_p, and axial strain, ε_a, when q_p was obtained are summarized in Table 2. Fig. 4 shows the

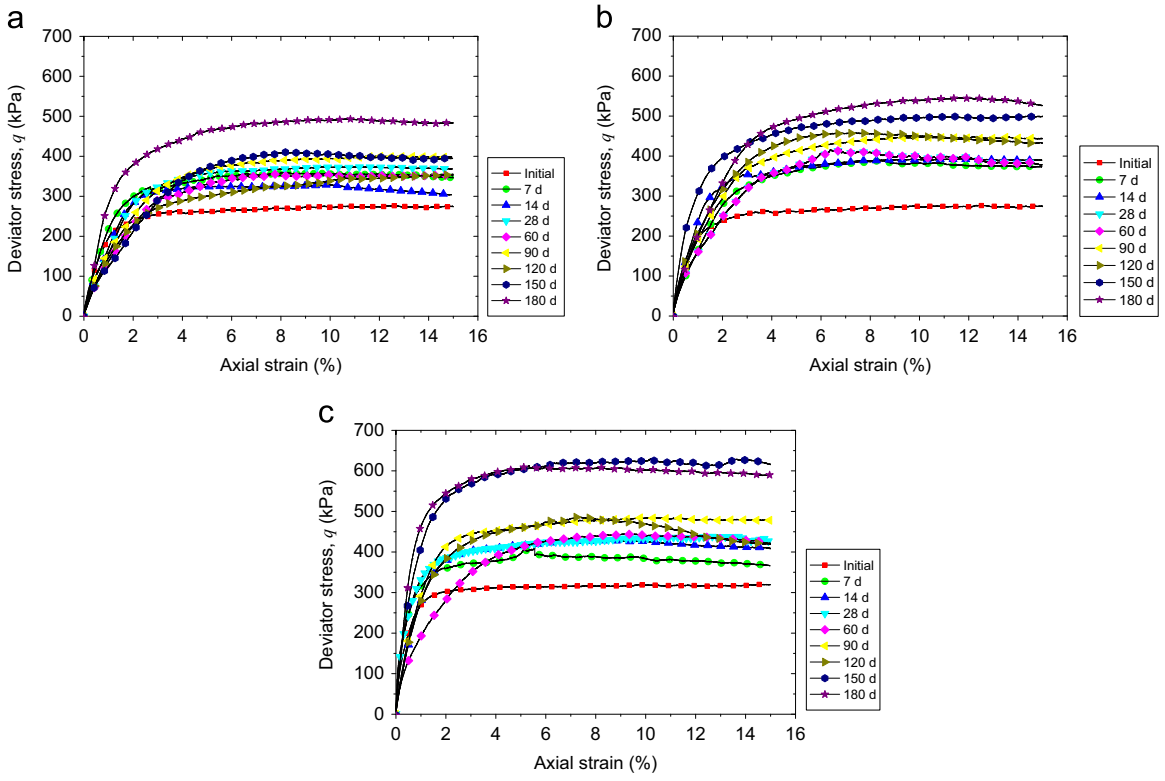

Fig. 4. Deviator stress versus axial strain under various confining pressures, σ_c; (a) σ_c= 50 kPa, (b) σ_c=100 kPa and (c) σ_c=150 kPa.

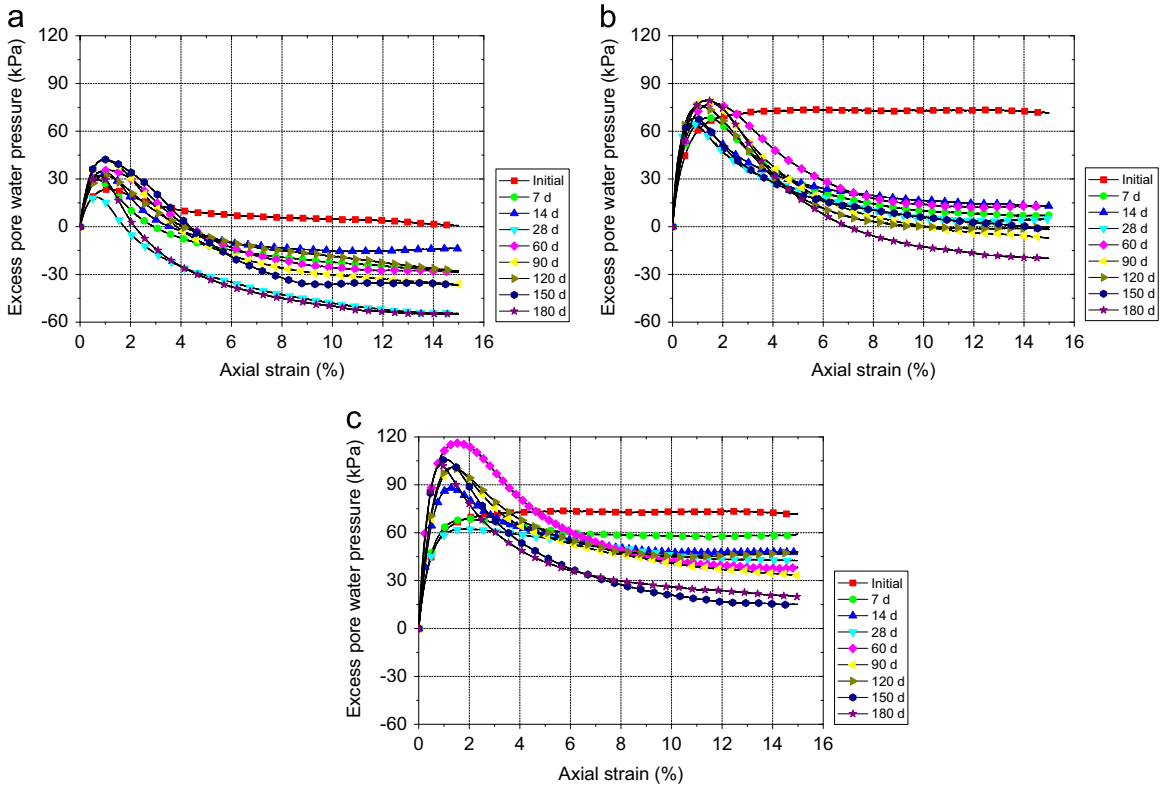

Fig. 5. Excess pore water pressure versus axial strain under various confining pressures, σ_c; (a) σ_c=50 kPa, (b) σ_c=100 kPa and (c) σ_c=150 kPa.

stress–strain curves for the specimens cured in the simulated leachate for different curing periods (0–180 days). Overall, the deviator stress, q, increased dramatically when ε_a was smaller than approximately 2%, and reached a peak after ε_a became 6% or more. After that, q remained almost constant until ε_a became 15%. The higher residual q was observed in specimens which had been cured for longer periods. For the cases of $\sigma_c = 50$ kPa (Fig. 4(a)), q_p at the initial state (0 day curing) was about 250 kPa, while q_p after curing in the simulated leachate ranged from 300–500 kPa. For the cases of $\sigma_c = 150$ kPa (Fig. 4(c)), q_p in the initial state was 300 kPa, while q_p after 180 days curing was increased to approximately 600 kPa, which was double the value of q_p at the initial state.

Fig. 5 show the results of excess pore water pressure (PWP) versus axial strain. For the initial state specimen under $\sigma_c = 50$ kPa, excess PWP showed an increasing trend until it reached a peak value (approximately 20 kPa), and then it decreased steadily to about 0 kPa at $\varepsilon_a = 15\%$. In contrast, under $\sigma_c = 100$ and 150 kPa, excess PWP increased and reached a maximum at $\varepsilon_a = 2\%$, and then maintained a constant value until ε_a reached 15%. The initial state specimens without curing displayed a contractive behavior in shearing process, in which the positive excess pore water pressure was maintained during shearing.

When the specimens cured in the simulated leachate, specimens of the higher σ_c and the longer curing period had the higher peak excess pore pressure. For the cases of $\sigma_c = 50$ kPa, excess PWP dramatically increased in the initial shearing stage which indicated a contractive behavior (see Fig. 5(a)). After reaching the peak value at ε_a of about 1%, excess PWP decreased to a negative value for all the specimens cured. For the specimen cured for 180 days, the peak excess PWP was about 40 kPa and the largest negative excess PWP was approximately -60 kPa. The increase in the negative excess PWP showed a dilatancy behavior of the waste mixture, which was induced by curing in the simulated leachate.

For the cases of $\sigma_c = 100$ kPa (Fig. 5(b)), specimens cured for more than 90 days also showed a dilatancy behavior, which was clearly indicated by the generation of negative excess PWP. The peak excess PWP was about 80 kPa and the largest negative excess PWP was approximately -20 kPa for the specimen cured for 180 days. The peak excess PWPs mobilized were almost twice as large as those obtained under $\sigma_c = 50$ kPa, while the negative PWPs was about one third as large as those under $\sigma_c = 50$ kPa.

For the cases of $\sigma_c = 150$ kPa (Fig. 5(c)), excess PWP profiles similar to those for $\sigma_c = 50$ and 100 kPa were obtained. However, the excess PWP profile for the 7 days curing specimen was similar to that at the initial state, which did not indicate any dilatancy behavior.

From the stress–strain relationships and excess PWP profiles obtained in CU tests, the shear strength of the waste mixture increased by curing due to changes in microstructures, which was indicated by PWP profiles. It can be considered that formation of hydration products filling the pores in the waste mixture fabric affected the PWP profiles. Since the specimens with the denser structure had a higher dilatancy, larger negative excess PWPs were generated, which led to the higher residual strength in the specimens cured for longer periods of time.

3.1.2. Stress-path of waste mixture with curing time

The deviator stress, q, and the mean effective stress, p', are calculated by following Eqs. (1) and (2):

$$q = \sigma_1' - \sigma_3' \tag{1}$$

$$p' = \left(\sigma_1' + 2\sigma_3'\right)/3 \tag{2}$$

where σ_1' and σ_3' are the effective axial and confining stress. The effective stress paths were plotted in a p' plane as shown in Fig. 6. The effective stress paths showed a similar shape except for some cases under $\sigma_c = 150$ kPa. From the initial point, the stress paths showed a decrease in p, which shifted to the left with the generation of excess PWP. After the PWP reached its peak, p' started to increase, and the stress paths shifted to the right. As the shearing proceeded, the higher q' was observed under a certain p' for specimens cured for longer periods of time. After q' reached its peak, softening behavior was observed in all but the specimens which had not been subjected to curing.

3.1.3. Deformation modulus of waste mixture with curing time

The deformation modulus was determined from the stress–strain curves. Since the stress–strain curves obtained were nonlinear, the deformation modulus was calculated by following the procedure proposed by Kondner (1963), in which the stress–strain curve can be represented by hyperbolic equations:

$$\sigma_1' - \sigma_3' = \frac{\varepsilon_a}{a + b\varepsilon_a} \tag{3}$$

Eq. (3) can also be rewritten as:

$$\frac{\varepsilon_a}{\sigma_1' - \sigma_3'} = a + b\varepsilon_a \tag{4}$$

A plot of $\varepsilon_a/\left(\sigma_1' - \sigma_3'\right)$ versus ε_a is subjected to a straight line with a slope, b, and an intercept, a, with the ordinate. Deformation modulus, E, is given by Eq. (5).

$$E = 1/a \tag{5}$$

Table 3 shows the E values determined for all the cases, which vary between 25 and 65 MPa. The deformation modulus, E, depended primarily on σ_c, as observed in typical dense sand. In addition, although some exceptions existed in the lower σ_c cases, E increased with the curing period. Fig. 7 shows the relationship between E and the curing period for $\sigma_c = 150$ kPa. E after curing for 180 days was about twice as large as that of the specimen which had not been cured. The increase in the deformation modulus with curing is consistent with other studies for stabilized soil, sand and bottom ash (Åhnberg 2007; Baxter and Mitchell, 2004; Kim and Do 2012; Schmertmann 1991). Schmertmann (1991) also reported that the modulus increased with ageing in the case of cohesive samples.

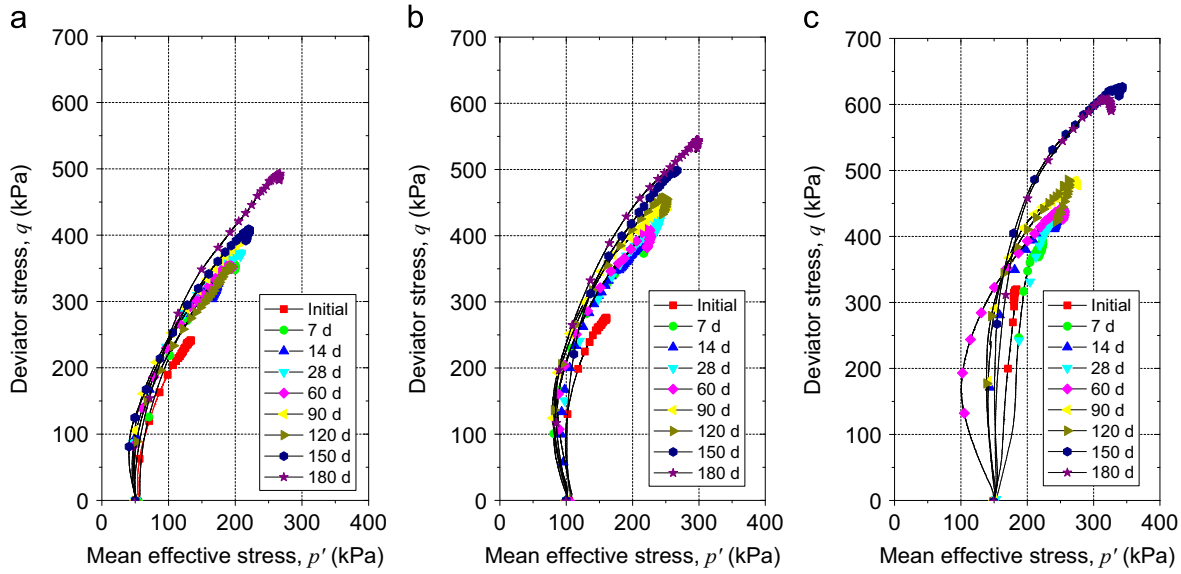

Fig. 6. Effective stress paths under various confining pressures, σ_c. (a) σ_c=50 kPa, (b) σ_c=100 kPa and (c) σ_c=150 kPa.

Table 3
Deformation modulus determined in the CU tests.

Curing period (days)	Deformation modulus (MPa)		
	σ'_3=50 kPa	σ'_3=100 kPa	σ'_3=150 kPa
0	25.8	28.3	32.2
7	39.2	37.7	40.6
14	32.4	41.0	42.7
28	40.2	43.5	44.5
60	39.0	42.4	47.2
90	44.3	48.8	50.1
120	39.0	46.7	44.8
150	45.9	52.3	64.4
180	52.3	60.4	60.6

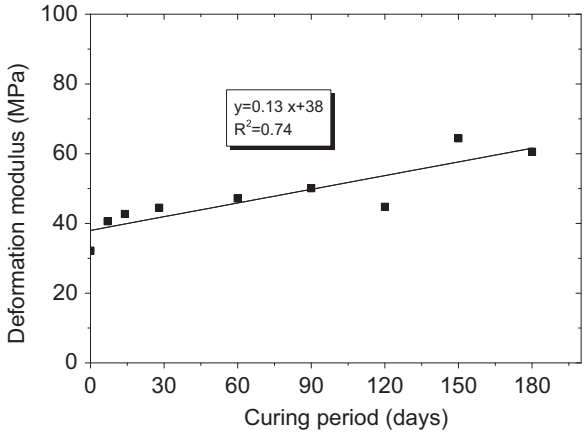

Fig. 7. Deformation modulus versus curing period at σ_c=150 kPa.

3.2. Hydraulic conductivity of waste mixture with curing time

Hydraulic conductivity (k) values with the curing period are presented in Table 4. Hydraulic conductivity values showed a decreasing trend according to the curing period. k of the waste mixture decreased by one order of magnitude from 4.2×10^{-4} cm/s to 5.9×10^{-5} cm/s after curing for 180 days. The range of k is similar to the k values of municipal solid waste incinerator ash deposit determined by Itoh et al. (2005).

Table 4
Hydraulic conductivity test results.

Curing period (days)	Hydraulic conductivity k (cm/s)
0	4.2×10^{-4}
7	3.6×10^{-4}
14	2.1×10^{-4}
28	4.6×10^{-4}
60	3.0×10^{-4}
90	3.0×10^{-4}
120	2.9×10^{-4}
150	2.7×10^{-4}
180	5.9×10^{-5}

Towhata et al (2010) carried out hydraulic conductivity tests on incinerator ash samples submerged in water, and also confirmed a decreasing trend in hydraulic conductivity with curing through generation of cementations products with which the pore of the sample was filled. However, neither the cement generation processes nor the type of products generated were specified. In this research, to identify the processes to decrease the hydraulic conductivity of the waste mixture by curing, XRD and SEM analyzes were conducted as described in the following sections.

3.3. XRD analysis on waste mixture after curing

Fig. 8 show the XRD results for the specimens with various curing periods (0, 60, 90, 150 and 180 days). As shown in Fig. 8(a), peaks for calcite ($CaCO_3$), hydrated gypsum and quartz

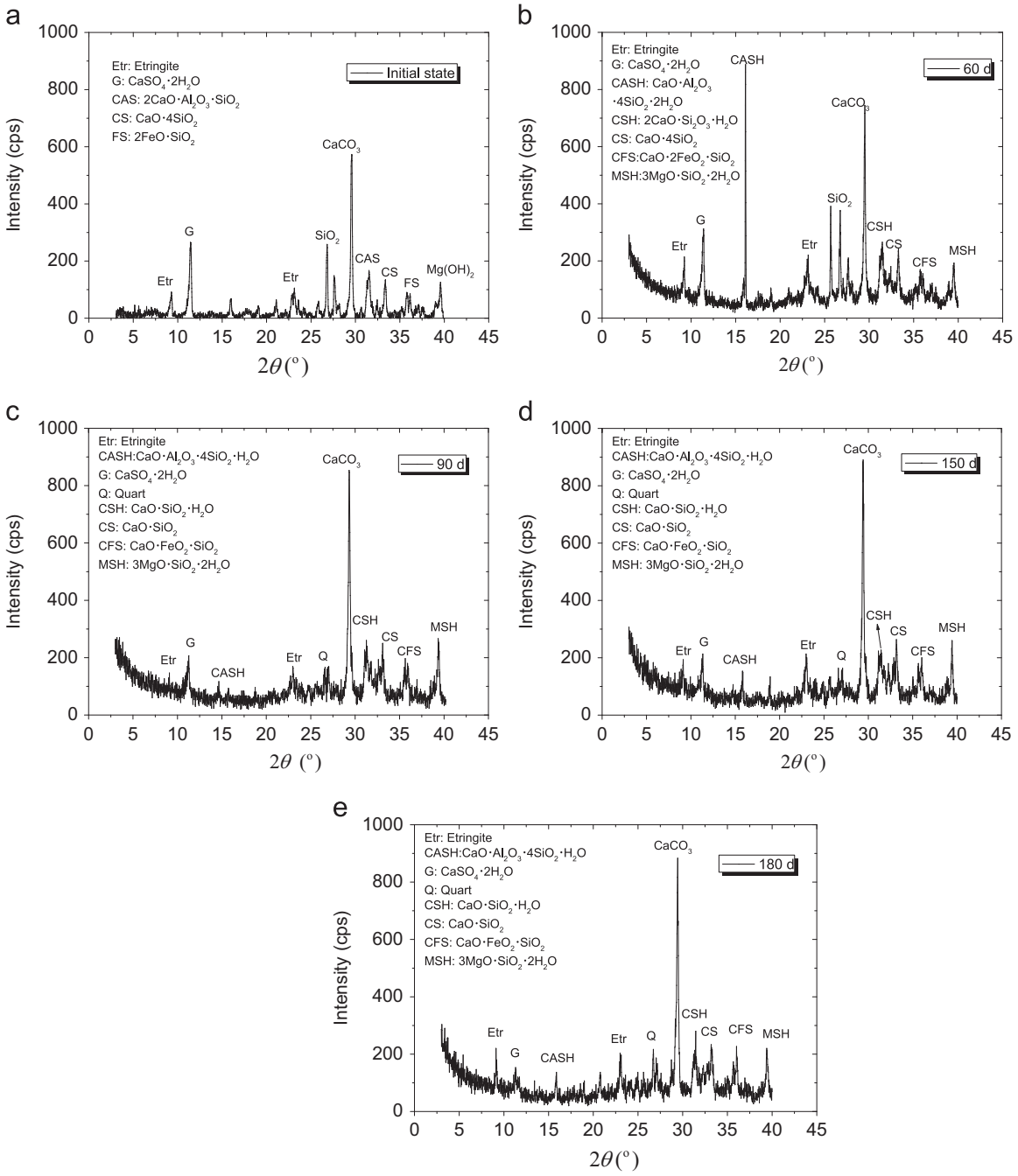

Fig. 8. XRD patters for the waste mixture with various curing periods; (a) 0 day (initial state), (b) 60 days, (c) 90 days, (d) 150 days and (e) 180 days.

were clearly observed in the specimen at the initial state. Calcite showed the highest intensity (about 580 cps at $2\theta = 29.4^{\circ}$). The intensity of the peaks for quartz and gypsum were reduced dramatically with the curing period. Since the simulated leachate contained chloride (Cl^-) and sulfate ions (SO_4^{2-}) as major anions, hydrated gypsum can be produced by the reaction with the calcium contained in the waste mixture described in Eq. (6).

$$Ca^{2+}\ (aq) + SO_4^{2-}(aq) + 2\ H_2O \rightarrow CaSO_4 \bullet 2H_2O \quad (6)$$

Further, hydrated gypsum can be transformed into ettringite in the waste mixture. Ettringite is one of the substances responsible for the strength development by cement-based solidification agents, and formation of ettringite is represented by the following reaction formulas:

$$3CaO \cdot Al_2O_3 + 3CaSO_4 32H_2O \rightarrow 3CaO \cdot Al_2O_3 \cdot 3CaSO_4 \cdot 32H_2O \quad (7)$$

$$4CaO \cdot Al_2O_3 \cdot Fe_2O_3 + 6CaSO_4 + 2Ca(OH)_2 + 62H_2O \rightarrow 3CaO \cdot Al_2O_3 \cdot 3CaSO_4 \cdot 32H_2O + 3CaO \cdot Fe_2O_3 \cdot 3CaSO_4 \cdot 32H_2O \quad (8)$$

The largest peak of ettringite ($2\theta = 9.2^{\circ}$) was detected for the sample after 180 days curing. Kamon and Nontananandh

(1990) inferred that the formation of ettringite ($3CaO \cdot Al_2O_3 \cdot 3CaSO_4 \cdot 32H_2O$) caused a significant decrease in moisture content by combining a large amount of water molecules in its crystals, leading to early strength development in stabilized soil.

The formation of hydration products is expected to contribute to the increase in shear strength of soils. Fig. 8(a) also indicated the presence of hydration products such as calcium silicate hydrate, $CaO \cdot SiO_2 \cdot H_2O$ (CSH) and $CaO \cdot Al_2O_3 \cdot SiO_2 \cdot H_2O$ (CASH). In previous studies, the formation of these hydration products, which was verified by XRD and SEM observations, was considered a primary factor in the development of the strength of lime or cement stabilized soil (Kamon and Nontananandh 1990; Rajasekaran 2005; Rajasekaran et al. 1997). Similarly, the formation of hydration products can be seen in Figs. 8(b)–(e) with significant changes in the XRD patterns. As illustrated in these figures, the XRD patterns of the samples cured for 60, 90, 150, and 180 days included several new peaks which did not appear in the samples at the initial state. These new peaks indicated the presence of hydration products such as CSH at $2\theta = 31.3^\circ$ and CASH at $2\theta = 15.8^\circ$. In a number of earlier studies on stabilized soil, the authors

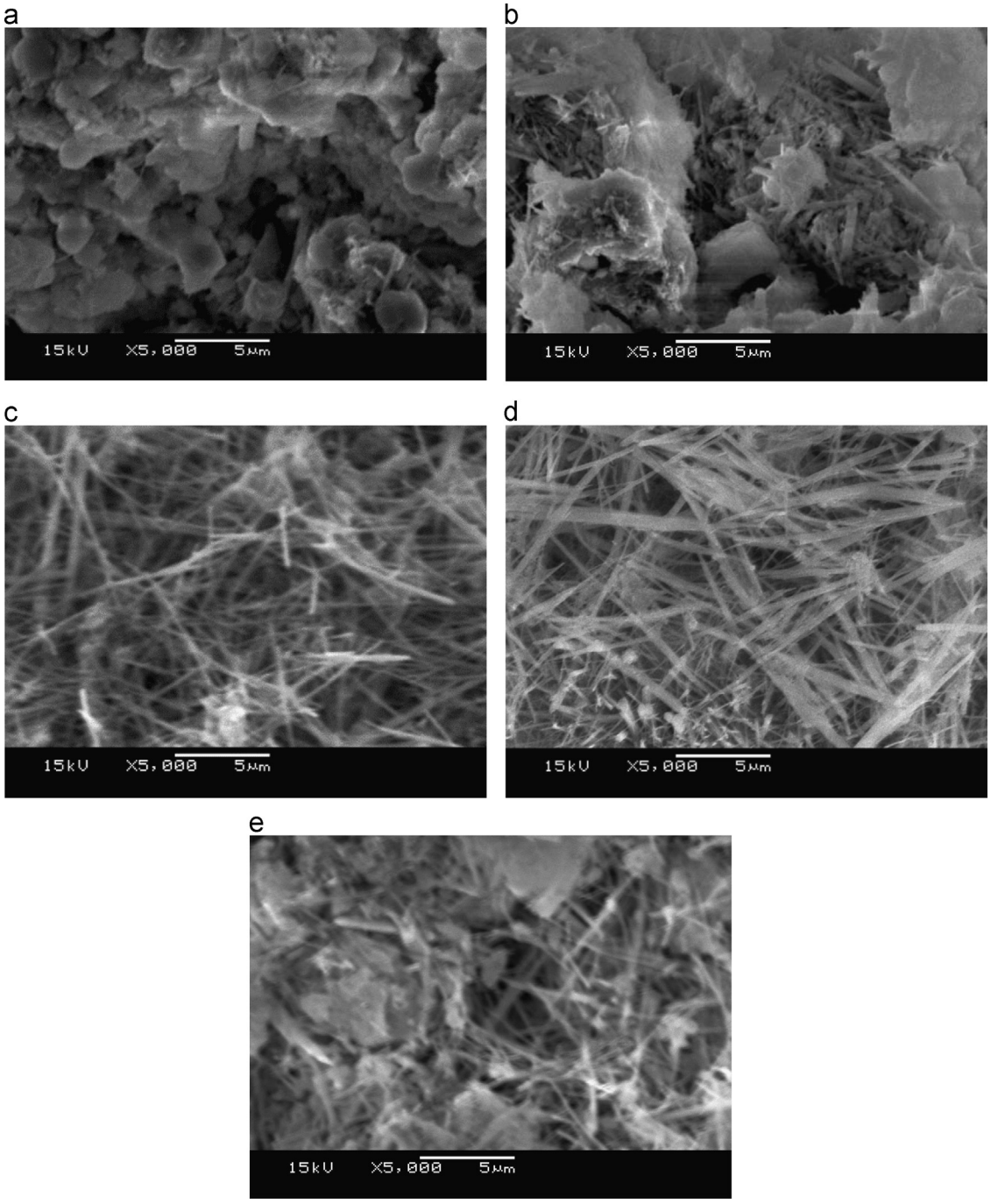

Fig. 9. SEM images for the waste mixture specimens with various curing periods; (a) 0 day (initial state) (b) 60 days, (c) 90 days,(d) 150 days, and (d) 180 days.

indicated that the increase in the amount of hydration products such as CSH contributed to the strength development of stabilized soil, and the strength increment was in correspondence with XRD intensities of CSH products (Ariizumi 1977; Kamon et al. 2001; Kamon and Nontananandh 1990).

3.4. SEM image analysis of waste mixture after curing

Fig. 9(a) shows the microstructure of waste mixture immediately after molding without curing. The main components at the initial state were numerous irregular particles.

The SEM images with a magnitude of 5000 for the samples that were cured for 60, 90, 150, and 180 days are shown in Figs. 9(b)–(e), respectively. There was a clear difference, compared with the initial state; the presence of needle-like ettringite can be easily observed in the samples cured for longer periods of time. The presence of ettringite that fills up the voids in the waste mixture structure strengthens the bonding between waste particles. As a result, the formation of these products led to an increase in the peak deviator stress and a decrease in hydraulic conductivity of the waste mixture after curing.

3.5. Aging effects on mechanical properties of the waste mixture

The relationships between the stress ratio, q/p', and the axial strain, ε_a, obtained in the CU tests were illustrated in Fig. 10. Under $\sigma_c = 50$ kPa, while the peak q/p' value was about 1.8 for the initial specimen, peak q/p' values were gradually increased and reached about 2.5 after 150 and 180 days of curing. For $\sigma_c = 100$ kPa, the peak q/p' values increased from 1.6 at the initial state to about 2.5 after curing for 180 days. A similar trend was also observed under $\sigma_c = 150$ kPa, although the peak q/p' values slightly decreased. However, the q/p' values at the residual state for the larger ε_a were almost constant (about 1.8), regardless of the curing periods and confining pressures. These observations indicated that there were no changes in the cohesion or friction angles in the specimen cured in simulated leachate. The effects of curing are clearly observed only in the small strain region and the higher q/p' values were mobilized by curing. However, in the large strain region, the residual q/p' was almost constant and not influenced by curing. This indicates a kind of overconsolidation effect was mobilized by aging. Athanasopoulos (1993) presented that the overconsolidation ratio increases linearly with the duration of aging for remolded clay. The q/p'-strain curves for the waste mixture after curing is consistent with those presented by Åhnberg (2007) for overconsolidated stabilized soil. The author pointed out that the specimens of stabilized soil exhibited the brittle behavior, with a significant reduction in strength after failure under the undrained condition.

The relation between q_p and the curing periods under $\sigma_c = 150$ kPa is shown in Fig. 11. The q_p values were well correlated with the curing period, and the q_p of the specimen after 180 days curing was twice that of the initial state. As shown in Fig. 4, the q_p was obtained when ε_a was larger than 6%. Considering that the q/p' are almost constant when ε_a were more than 6% (Fig. 11), the higher q_p values can be attributed to the smaller excess PWP generated in the specimens after curing

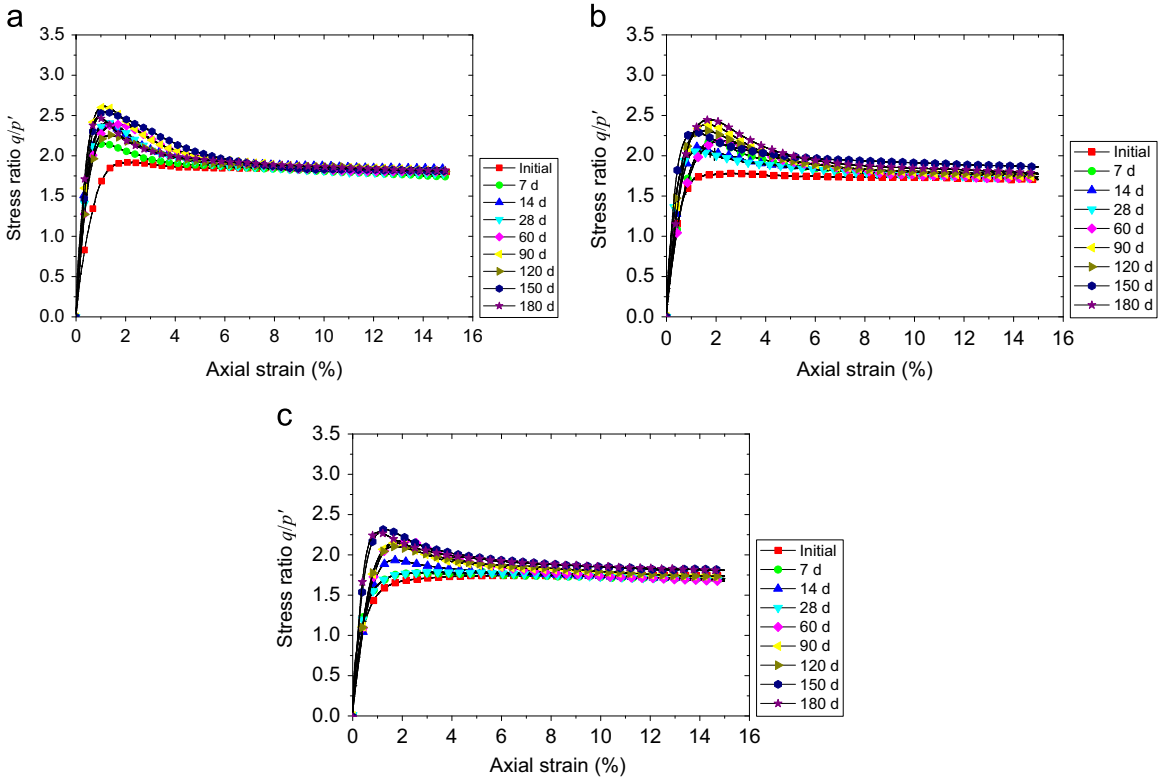

Fig. 10. Stress ratio q/p' versus axial strain; (a) $\sigma_c = 50$ kPa, (b) $\sigma_c = 100$ kPa, and (c) $\sigma_c = 150$ kPa.

(see Fig. 5), which is influenced by changes in the microstructure due to the generation of hydration products during curing. In addition, the structure of the waste mixture was densified due to the pozzolanic reactions that cause the formation of hydration products (ettringite and CSH) and, in turn, fill the pore spaces contributing to an increase in shear strength. The dry density of the waste mixture specimens that were cured in the simulated leachate slightly increased from 1.02 to 1.03 after 14 days to 1.05 to 1.25 after 180 days (see Table 2). Therefore, the development of q_p with the curing period was explained by these changes in the microstructure. The XRD and SEM results support these changes in the microstructure of the waste mixture as described in the above sections. The XRD intensities for ettringite versus q_p of the waste mixture samples are plotted in Fig. 12. The shear strength of the waste mixture shows an incremental trend with the XRD intensity of ettringite.

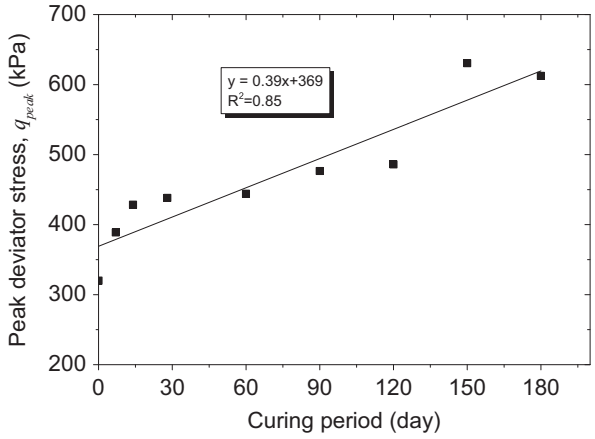

Fig. 11. Peak deviator stress versus curing period at σ_c=150 kPa.

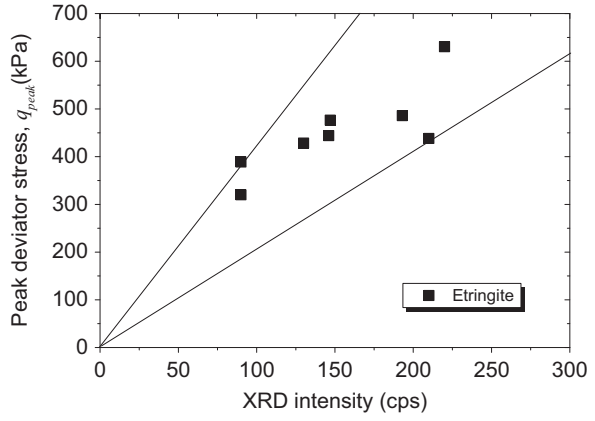

Fig. 12. Relation between peak deviator stress, q_p, and XRD intensity of ettringite.

From these discussions, the expected process affecting the undrained shear behavior of the waste mixture can be summarized in Fig. 13. When the waste mixture was submerged in the simulated leachate, hydrated gypsum and ettringite were formed primarily. After that, the pozzolanic reactions took place, generating hydration products such as CSH. As a result, the micropore structure of the waste mixture became densified by the generation of hydration products, as observed by the SEM and XRD analyzes. These processes were verified by the changes in the dry density and hydraulic conductivity induced by curing. The densification of the waste mixture samples led to an increase in the negative pore pressure during shearing due to the dilatancy effect, which is more likely to occur in the specimens cured for the longer periods. However, considering that q/p' in the residual state are almost constant regardless of the curing period, the higher q_p is attributed to the higher p' mobilized by the generation of negative excess PWP. Thus, the excess PWP profiles play a major role in the increase in q_p of the waste mixture.

4. Practical implications

The shear strength parameters are important for evaluating the stability of the waste layer in coastal landfills. In this research, the aging effects on the undrained shear strength of the waste mixture were studied and the results showed that the

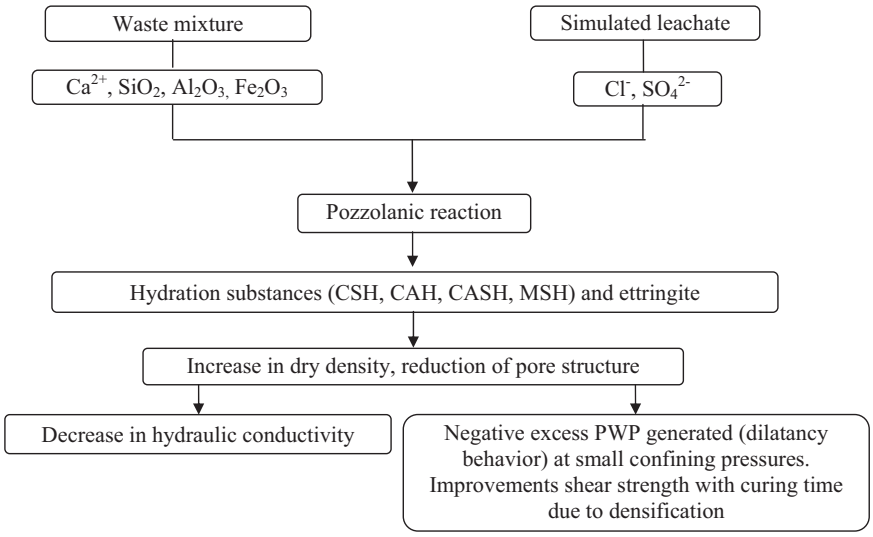

Fig. 13. Expected processes affecting the undrained shear behavior and hydraulic conductivity of the waste mixture cured in the simulated leachate.

peak deviator stress increased with the curing periods. The shear strength of the waste samples ranged from about 300 kPa to 600 kPa under $\sigma_c = 150$ kPa, since the peak deviator stress were primarily influenced by the changes in excess PWP profiles. Accordingly, the peak q/p' values around $\varepsilon_a = 1\%$ increase by a kind of overconsolidation effect after curing but the residual q/p' values do not change, regardless of the confining pressures and curing periods. Therefore, the significance of aging effects depends on whether to employ peak or residual strength in practical design.

Another important factor in the post-closure use of a coastal landfill site is the bearing capacity of the waste mixture layer. The bearing strength capacity required for typical structures, such as residential houses, is 100–200 kPa or 15–30 in SPT-N value according to the Japan Waste Management Consultant Association (JWMCA 1994). The test results showed that waste mixture exhibited a self-hardening behavior in the leachate with a shear strength higher than 200 kPa.

5. Conclusions

This study investigated the aging effects of the waste mixture, which was mainly composed of incinerator ash, slag, and surplus soil, on the undrained shear behaviors and hydraulic conductivity, for the future post-closure utilization of a coastal landfill site. The main conclusions derived from the results of laboratory experiments can be summarized as follows.

1) Waste mixture samples were cured by submerging in the simulated leachate and cured in maximum 180 days. The initial and cured samples were subjected to CU triaxial compression tests. The results showed that both the peak shear strength and the dilatancy of the waste mixture increased with the curing time. The processes responsible for this behavior could be explained by the changes in microstructure of the waste mixture, which was densified through formation of hydration products (ettringite and CSH), and the generation of negative excess PWP. The densification of the waste mixture samples associated with curing led to an increase in the negative pore pressure during shearing due to the dilatancy effect. Accordingly, the higher q_p is attributed to the higher p' mobilized by the generation of negative excess PWP. However, the q/p' values at the residual state for the larger ε_a were almost constant (about 1.8), regardless of the curing periods and confining pressures. These observations indicated that there were no changes in cohesion and friction angles induced by curing in the simulated leachate. It can be considered that a kind of overconsolidation effect was mobilized by aging only in the small strain region.
2) The results of the SEM and XRD analyzes verified that the formation of ettringite and other hydration products, such as CSH, was promoted by curing. The formation of these products led to the changes in microstructures of the waste mixture, which was also supported by a decrease in hydraulic conductivity with curing.
3) Waste mixture samples showed an increase in the deformation modulus with curing time. This trend was consistent with the increase in undrained shear strength of waste mixture samples. Therefore, the waste mixture layer investigated in this study could be possibly used as foundation layers with its sufficient bearing capacity in post-closure use of coastal landfill sites.

Acknowledgments

This work was supported by JSPS KAKENHI Grant number 25289145. The authors wish to acknowledge the scholarship provided to the first author's study in Japan by the Ministry of Education and Training of Vietnam. The authors are grateful to Dr. Hermelinda Plata and Dr. Atsushi Takai (Kyoto University) for their helpful comments and suggestions.

References

Aburatani, S., Hayashi, Y., Nishikawa, T., 1996. Offshore waste disposal by Osaka Bay Phoenix project. In: Kamon, M. (Ed.), Environmental Geotechnics. Balkema, Rotterdam,Netherlands, pp. 623–628.

Åhnberg, H., 2007. On yield stresses and the influence of curing stresses on stress paths and strength measured in triaxial testing of stabilized soils. Can. Geotech. J. 44 (1), 54–66.

Araike, H., Kambara, H., Maeda, H., Nonami, S., Watanabe, Y. (2010). Physical and density characteristics of Kobe offshore reclamation disposal site. In: Proceedings of the 45th Japan National Conference on Geotechnical Engineering, pp.471-472 (in Japanese).

Ariizumi, M., 1977. Mechanism of lime stabilized soil. Soil. Found. 227, 9–15.

Athanasopoulos, G., 1993. Effects of ageing and overconsolidation on the elastic stiffness of a remoulded clay. Geotech. Geoenviron. Eng. 11 (1), 51–65.

Baxter, C., Mitchell, J., 2004. Experimental study on the aging of sands. J. Geotech. Geoenviron. Eng. 130 (10), 1051–1062.

Doi, Y., Shigeyoshi, I., Yamada, M., 2000. Change of the mechanical properties of MSW-incinerated ash with the lapse of time. Proc. JSCE, 103–112.

Itoh, T., Towhata, I., Kawano, Y., Kameda, M., Fukui, S., Koelsch, F., and Yonai, Y., (2005). Mechanical properties of municipal waste deposits and ground improvement. In: Proceedings of the 16th International Conference on Soil Mechanics and Geotechnical Engineering, Millpress Science Publishers, Rotterdam, pp. 2273-2276.

JIS A 1204, 2009. Test Method for Particle Size Distribution of Soils, Japanese Industrial Standards Committee.

JIS A 1210, 2009. Test Method for Soil Compaction Using a Rammer, Japanese Industrial Standards Committee.

JGS 0051, 2009. Method of Classification of Geomaterials for Engineering Purposes, Japanese Geotechnical Society.

JGS 0520, 2009. Preparation of Soil Speciments for Triaxial Tests, Japanese Geotechnical Society.

JGS 0523, 2009. Method for Consolidated-undrained Triaxial Compression Tests on Soils with Pore Water Pressure Measurements, Japanese Geotechnical Society.

JWMCA, 1994. Research Report on Landfill Stabilization,Japan Waste Management Consultant Association.

Kamon, M., Gu, H., I, M., 2001. Improvement of mechanical properties of ferrum lime stabilized soil with the addition of aluminum sludge. Mater. Sci. Res. Int. 7 (1), 47–53.

Kamon, M., Nontananandh, S., 1990. Contribution of stainless-steel slag to the development of strength for seabed hedoro. Soil Found. 30 (4), 60–72.

Kim, Y.T., Do, T.H., 2012. Effect of bottom ash particle size on strength development in composite geomaterial. Eng. Geol. 139–140 (0), 85–91.

Kondner, R.L., 1963. Hyperbolic stress–strain response: cohesive soils. J. Soil Mech. Found. Eng. Div., ASCE 189 (1), 115–143.

Rad, N.S., Clough, G.W., 1984. New procedure for saturating sand specimens. J. Geotech. Eng. 110 (9), 1205–1218.

Rajasekaran, G., 2005. Sulphate attack and ettringite formation in the lime and cement stabilized marine clays. Ocean Eng. 32 (8–9), 1133–1159.

Rajasekaran, G., Murali, K., Srinivasarashavan, R., 1997. Effect of chlorides and sulphated on lime treated marine clays. Soil Found. 37 (2), 105–115.

Sato, K., Matsumura, K., Yoshida, N., Shimaoka, T., Miyawaki, K., Hanashima, M., 2001. Dynamic characteristics of incineration residue under different curing conditions. In: Proceedings of the 4th JGS Symposium on Environmental Geotechnics, Japanese Geotechnical Society, pp. 55–58, (in Japanese).

Schmertmann, J., 1991. The mechanical aging of soils. J. Geotech. Eng. 117 (9), 1288–1330.

Shimaoka, T., Zhang, R., Watanabe, K., 2007. Alterations of municipal solid waste incineration residues in a landfill. Waste Manag. 27 (10), 1444–1451.

Towhata, I., Imai, Y., Uno, M., 2010. Improvement of MSW subsoil for mechanical stabilization and urban use. In: Geotechnics, M., Datta, R.K., Srivastava, G.V., Ramana, Shahu, J.T. (Eds.), Proceedings of the 6th International Congress on Environmental. Tata McGraw Hill, New Delhi, pp. 318–327.